Comparison between transfer path analysis methods on an electric vehicle

COMPARISON BETWEEN TRANSFER PATH ANALYSIS METHODS ON AN ELECTRIC VEHICLE

A. Diez-Ibarbia[1], M. Battarra[2], J. Palenzuela[3], G. Cervantes[3], S. Walsh[5*], M. De-la-Cruz[4], S. Theodossiades[4] and L. Gagliardini[6]

[1]*Structural and Mechanical Engineering Department. University of Cantabria. Avda. Los Castros s/n - 39007, Santander, Spain.*

[2] *Engineering Department. University of Ferrara. Via Saragat, 1 - 44122, Ferrara, Italy.*

[3]*Mechanical Engineering and Energy. Miguel Hernández University. Avda. de la Universidad, s/n - 03202, Elche, Spain.*

[4]*School of Mechanical and Manufacturing Engineering. Loughborough University, Loughborough LE11 3TU, UK.*

[5]*Department of Aeronautical & Automotive Engineering. Loughborough University. Loughborough LE11 3TU, UK.*

[6]*PSA-Peugeot-Citroen. Route de Gisy 78943, Velizy-Vilacoublay, France.*

* Corresponding author.
Dr. Stephen Walsh
E-mail address: S.J.Walsh@Lboro.ac.uk

Abstract

A comparison between transfer path analysis and operational path analysis methods using an electric vehicle is presented in this study. Structure-borne noise paths to the cabin from different engine and suspension points have been considered. To realise these methods, two types of test have been performed; operational tests on a rolling road and hammer tests in static conditions. The main aim of this work is assessing the critical paths which are transmitting the structure-borne vibrations from the electric vehicle's vibration sources to the driver's ear. This assessment includes the analysis of the noise contribution of each path depending on the frequency and vehicle speed range and moreover, the assessment of the path noise impact for harmonic orders which arise due to the physical components of the electric vehicle. Furthermore, the applicability of these methods to electric vehicles is assessed as these techniques have been extensively used for vehicles powered with internal combustion engines.

*Keywords***:** Noise path analysis, acoustic pressure, electric vehicle, operational test, impact test

1. Introduction

In the last decades, the regulatory requirements on the automotive sector have been made gradually stricter in environmental matters (Official Journal of the European Communities, 1991; 1994; 2002; 2007), in addition customers are demanding cheaper ways of transport (Official Journal of the European Union, 2008; Taymaz & Benli, 2014). These are the reasons why on the one hand, automotive companies have shown a keen interest in improving the energy efficiency in petrol and diesel engine vehicles and, on the other hand, alternative ways of producing energy that replaces or decreases the petrol and diesel fuel consumption have been looked for (Chan, 1993; Chan, 2002; DeLuchi, 1989; El-Refaie, 2011; Fukuo et al., 2001; Taymaz & Benli, 2014; Thanapalan et al., 2011). In this framework, hybrid vehicles (HV) and electric vehicles (EV) are two of the technological approaches adopted. These types of vehicle present the advantage that they pollute the environment less than other conventional technology-based vehicles (El-Refaie, 2011; Fukuo et al., 2001; Judd & Overbye, 2008; Taymaz & Benli, 2014), nevertheless one issue of concern has been the noise impact that they incur (Ahlersmeyer, 2009; De Klerk & Ossipov, 2010; Elliott et al., 2013; Gajdatsy et al., 2009; Guasch et al., 2013;

Lennström et al., 2014; Plunt, 2005). In this regard, whilst the radiated noise in the exterior of these vehicles is almost non-existent in low-speed regime, the interior noise does not fulfil high standards in terms of comfort. The former can cause accidents with pedestrians and the latter could make the potential customer reluctant to purchase the vehicle. Hence, resolving these noise issues is of crucial importance.

In this framework, the interest on Noise, Vibration and Harshness (NVH) has been growing over time, turning out to be one of the main areas related to the customer perception of quality in vehicles. In the open literature (De Klerk & Rixen, 2010; De Klerk & Ossipov, 2010; Gajdatsy et al., 2009; Janssens et al., 2011; Lennström et al., 2014; Magrans, 1981; Magrans, 1993; Padilha & De Frana Arruda, 2006), various approaches have been reported in order to define the passive transfer paths that vibrations or acoustic signals use to propagate through the vehicle. One of these methods, the Transfer Path Analysis (TPA), was first developed in the early '80s and was seen as a tool to improve the NVH performance of several systems. This method has the main goal of reducing and improving the noise perceived in the cabin by the driver and the rest of occupants in the vehicle (Ahlersmeyer, 2009; De Klerk & Ossipov, 2010; Elliott et al., 2013; Plunt, 2005). Following this procedure, it is possible to measure the effect, in terms of noise or vibration that a source is producing, on a receiver and to determine which structure/air-borne paths are utilised. As a matter of fact, this method determines the relationship between the input generated by the sources and the receiver output. Depending on these inputs and outputs, different TPA variations can be applied. Eventually, it becomes possible to assess in which path a modification should be implemented in order to improve the system behaviour, considering the vehicle speed and frequency conditions that have to be refined. The strengths of this approach are the ease of validating the results and the fact that cross-coupling effects between paths are always considered. Ideally ,the latter should be small or even negligible, which means that the influence of a force applied on a specific point must be maximum at the application point, with the other force contributions being negligible compared to this one (Janssens et al., 2011).

Classical TPA was seen as a useful method to improve the NVH performance of different systems e.g. cars, aircrafts and boats; nevertheless some weaknesses in the method and the need for quicker methods led researchers to develop new techniques entirely based upon *in-situ* measurements (De Klerk & Ossipov, 2010; De Sitter et al., 2010; Gajdatsy et al., 2009; Gajdatsy et al., 2010; Janssens et al., 2011; Maia et al., 2001). New procedures similar to this technique but following different methodologies have been developed over the last years, such as the Operational Path Analysis (OPA) and Operational Path Analysis with exogenous inputs (OPAX). Among these methods, the classic OPA is the quickest method to implement but the validity of its results is difficult to assess (De Klerk & Ossipov, 2010; Gajdatsy et al., 2010; Maia et al., 2001), thus the lack of reliability of this technique is one of its weaknesses. Furthermore, in order to obtain accurate results with this approach, low cross-coupling is required and all the active paths must be considered in the analysis. From the literature (De Sitter et al., 2010), a variation of the OPA based on the indirect application of transmissibility concepts has been developed, although its applicability on a vehicle has still to be proven**.** With regard to OPAX, which is a method that evolved from the TPA and OPA methods, it has the novelty of using a parametric model to estimate the operational loads (Janssens et al., 2011). This approach claims to be more accurate than other load calculation methods in TPA, such as the dynamic stiffness method. Nonetheless, this OPAX method is more expensive in terms of execution time than the OPA method.

Despite the fact that the classical OPA method (direct transmissibility concept) has shown some limitations due to the requirement of considering all the paths and using low-coherence among the signals, the automotive

industry is strongly interested in implementing it because of the possibility of obtaining TPA-like results much quicker. The main advantage that OPA presents with respect to the other methods is that there is no need to identify the interface loads. Therefore, as the Frequency Response Functions (FRFs) are not necessary, the classical OPA is a quicker and less complex method based on the measurement/calculation of the transmissibility functions in operational tests (static tests are not required).

In this paper, a comparison between classic TPA and OPA methods in an EV has been made, taking into account the structure-borne noise introduced to the cabin from the motor mounts and the suspension points. The strengths and weaknesses of each method are presented. The hypothesis that the motor and suspensions (road) generate most of the acoustic noise in the cabin is also examined. Moreover, these TPA methods which are typically used for vehicles with internal combustion engines are now applied to an electric vehicle in this work. Hence, the versatility of these methods in an EV is assessed, which is the main novelty of this work.

The paper is divided in five sections. Section 2 provides the necessary background for the comprehension of the methods used in this study. In this section, the methodologies to develop the transfer path analysis are presented. In Section 3 the facilities and equipment used during the experimental tests as well as the description and layout of the different kinds of tests carried out in the study are described. In Section 4 the results of the two methods are assessed and compared, whilst in Section 5 the main conclusions are highlighted.

2. Methodology

The theoretical fundamentals of the TPA and OPA approaches are described in this section. With regard to these methods, the system to analyse is usually divided into a passive and an active part. The passive part contains the means that transmit the vibration and noise (paths) and the objects/people that absorb these vibrations (receivers), whilst the active part generates these fluctuations (sources) (Gajdatsy et al., 2010). Hence, the system could be divided on three different elements depending on their behaviour; sources, paths and receivers. The definitions of these three elements according to (Van der Seijs et al., 2016) are:

- Source: internal DoFs belonging to the active components that cause the operational excitation but are unmeasurable in practice
- Interface / passive paths: coupling DoFs residing on the interface between the active and the passive components
- Receiver: response DoFs at locations of interest on the passive component, possibly including acoustic pressures and other physical quantities

Particularly in this work, the electric vehicle (Figure 1) is therefore composed of: 1) sources, which generate the vibrations (the electric motor and the road); 2) receivers, which accept the noise (driver); and 3) transfer paths, as the structure-borne paths that the oscillations use to propagate themselves (mainly chassis and bodywork).

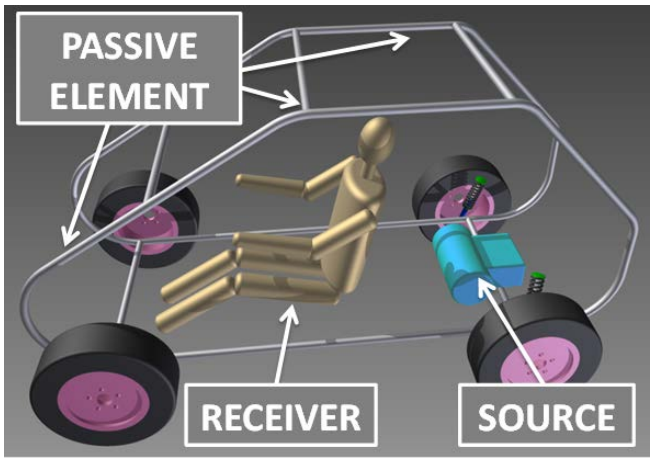

Figure 1 Illustration of the source-path-receiver system for an electric vehicle.

2.1 Transfer path analysis

Transfer Path Analysis is the classic method used to determine the relationship between the inputs, generated by the sources, and the receiver outputs. Depending on these inputs and outputs, different TPA approaches can be followed. In this study, as only structure-borne paths impact on the cabin is considered, the inputs are forces and the outputs are acoustic pressures. Since static tests are required to characterise the behaviour of each path, the model performance does not depend on the outcome of operational tests as in other approaches (such as OPA). Therefore, the key is to select the most important paths so that the behaviour of the model is close to reality. The validity of the results is determined by comparison between the real acoustic pressure values and the simulated ones. Another interesting aspect is that the cross-coupling effects, introduced when the engine is mounted, are always considered. Nonetheless, the execution time is higher than the OPA because many impact hammer tests (static tests) have to be performed in order to determine the FRFs.

TPA can be typically divided in three main stages: i) FRF measurements; ii) operational measurements; and iii) results and assessment (Gajdatsy et al., 2010; Gaudin & Gagliardini, 2007; Janssens & Britte, 2012). As the transfer matrix calculation method has been used in order to define the behaviour of the system, the first stage consists of performing static tests to obtain the force-to-acceleration FRFs in the transfer matrix ($H_i(\omega)$) and the force-to-acoustic pressure FRFs ($FRF_i(\omega)$) (Gajdatsy et al., 2010; Janssens et al., 2011).

$$H_i(\omega) = \begin{bmatrix} \frac{a_{11}^h}{f_1^h} & \cdots & \frac{a_{1n}^h}{f_n^h} \\ \vdots & \ddots & \vdots \\ \frac{a_{n1}^h}{f_1^h} & \cdots & \frac{a_{nn}^h}{f_n^h} \end{bmatrix} \quad (1)a$$

$$FRF_i(\omega) = \frac{p_i^h}{f_i^h} \quad (1)b$$

Where i is the path number, superscript h denotes a hammer test and a_i, f_i and p_i are the measured accelerations, forces and pressures. Recent studies (Lennström et al., 2016; Moorhouse et al., 2009; Van den Bosch et al., 2014) have highlighted the validity of "in-situ" measurements of the interface forces, fi. For the current study, the motor remained mounted to the vehicle body and, thus, the interface forces are correctly termed "blocked" forces.

The second stage (operational measurements) comprises run-up tests which are performed at a range of speeds of interest. In these tests, the operational forces are introduced to the system by the engine motion, while the operational accelerations and acoustic pressures are collected at the same points as in the FRF measurements. The blocked operational forces, $f_i(\omega)$, are calculated by means of the operational accelerations, $a_i(\omega)$, and the acceleration-to-force FRF transfer matrix $H_i(\omega)$:

$$f_i(\omega) = \begin{Bmatrix} f_1 \\ \cdots \\ f_n \end{Bmatrix} = H_i^{-1}(\omega) \cdot a_i(\omega) \quad (2)a$$

Once the blocked operational forces are known, the simulated acoustic pressure for each path, $p_i(\omega)$, can be calculated by these forces and the force-to-acoustic pressure FRFs. The pressure due to each path is then added together to provide a calculation of the total pressure, $p_C^{TPA}(\omega)$, in the interior cabin response point:

$$p_C^{TPA}(\omega) = \sum_{i=1,n} p_i(\omega) = \sum_{i=1,n} FRF_i(\omega) \cdot f_i(\omega) \quad (2)b$$

Where the superscript *TPA* refers to a TPA calculation and the subscript *C* refers to a calculated pressure.

Eventually, a comparison between the calculated and the corresponding operational acoustic pressure is conducted to assess the validity of the results.

A more detailed description of the methodology is provided in section 4.3.

2.2 Operational path analysis

From the literature (De Klerk & Ossipov, 2010; De Sitter et al., 2010; Gajdatsy et al., 2010; Maia et al., 2001), two different methods have been identified: the first one is based on the direct application of transmissibility concepts and the second one on an indirect application of these concepts. The latter has not been implemented in this paper because of applicability difficulties to the case of study. The operational path analysis with direct application of transmissibility concepts (hereinafter called OPA) has two main advantages (De Klerk & Ossipov, 2010; Gajdatsy et al., 2010; Maia et al., 2001). The first is that it is not necessary to calculate the loads that the engine introduces in the system since the transmissibility functions do not require them (only accelerations are necessary). The second advantage is that a large number of tests are not required (static tests are not performed), making this method the quickest and at the same time the least complex. Although this method is the easiest and quickest to perform, it might introduce issues because of the difficulties present in validation of its results. The first weakness is due to the estimation of the transmissibility matrix because the inverse acceleration matrix is needed. Moreover, unlike the TPA method, cross-coupling affects the transmissibility functions significantly. For this reason, low cross-coupling is compulsory to obtain reliable results (Gajdatsy et al., 2010). This method is also sensitive in terms of path consideration, thus all the main active paths must be considered so as to obtain reliable results. This occurs because the contributions of the missing paths are added to the measured ones. Therefore, if some of the main active paths are not considered, distorted results are obtained.

OPA can be divided in three main stages (Gajdatsy et al., 2010): i) operational measurements; ii) transmissibility function calculation; and iii) results and assessment. Operational measurements are performed in the same way as described for the TPA. With the accelerations of the body, $a_i^{1,2}(\omega)$, and the acoustic pressure

measurements in the cabin, $p_C^{1,OPA}(\omega)$, the transmissibility functions, $T_i(\omega)$, of each path related by equation (3):

$$p_C^{1,OPA}(\omega) = \sum_{i=1,n} T_i(\omega) \cdot a_i^{1,2}(\omega) \tag{3}$$

Where the superscripts 1, 2, OPA denote tests 1, 2 or OPA calculated, respectively. Finally, the obtained results are assessed, determining which transfer path is the most critical for a specific frequency. A full description of the methodology is provided in section 4.2.

3. Experimental measurements

In order to conduct both transfer path methods explained in the previous section, several experiments have to be carried out. More specifically, two common approaches (Ahlersmeyer, 2009; Padilha & De Frana Arruda, 2006) have been followed: static tests (in this case, hammer/impact tests) and dynamic tests (operational tests). On one hand, in the static tests, the accelerations and acoustic pressures are collected at the same time as a known force is applied in the points of interest. On the other hand, in the operational tests, the acceleration and noise are measured in the same locations as in the static tests but when the vehicle is in operation. Whilst the static tests were performed in a vehicle lifting bay using an impact hammer with a metallic tip, the operational tests required a chassis dynamometer where the dynamic experiments were performed. All the data gathered in this stage was post-processed to calculate the acceleration-to-force and force-to-acoustic-pressure FRFs.

Before the tests were performed, it was crucial to choose the path locations by analysing the layout of the vehicle's powertrain. The vehicle used was an electric car in which the most important feature is that the powertrain lays over the rear axis. For the sake of vehicle model simplicity and due to the available equipment, the eight paths assumed to be radiating the most structure-borne noise were identified. The first three locations (1-3) correspond to the three main powertrain mounts: in each location the vertical and longitudinal axes of the vehicle were considered for measurements. Two further measurement points (4, 5) have been considered at the locations where the rear suspension is supported in the vertical direction (these locations are shown in Figure 2 and labelled in Table 1).

Table 1 Location of the accelerometers installed and their directions on the vehicle.

LOCATION	MEASUREMENT POINT	DIRECTION	ACCELEROMETER LABEL	ASSOCIATED PATH
Engine mount 1	1	Vertical direction(Y)	1Y	1st
Engine mount 2	2	Vertical direction(Y)	2Y	2nd
Engine mount 3	3	Vertical direction(Y)	3Y	3rd
Suspension 1	4	Vertical direction(Y)	4Y	4th
Suspension 2	5	Vertical direction(Y)	5Y	5th
Engine mount 1	1	Axial direction (X)	1X	6th
Engine mount 2	2	Axial direction (X)	2X	7th
Engine mount 3	3	Axial direction (X)	3X	8th

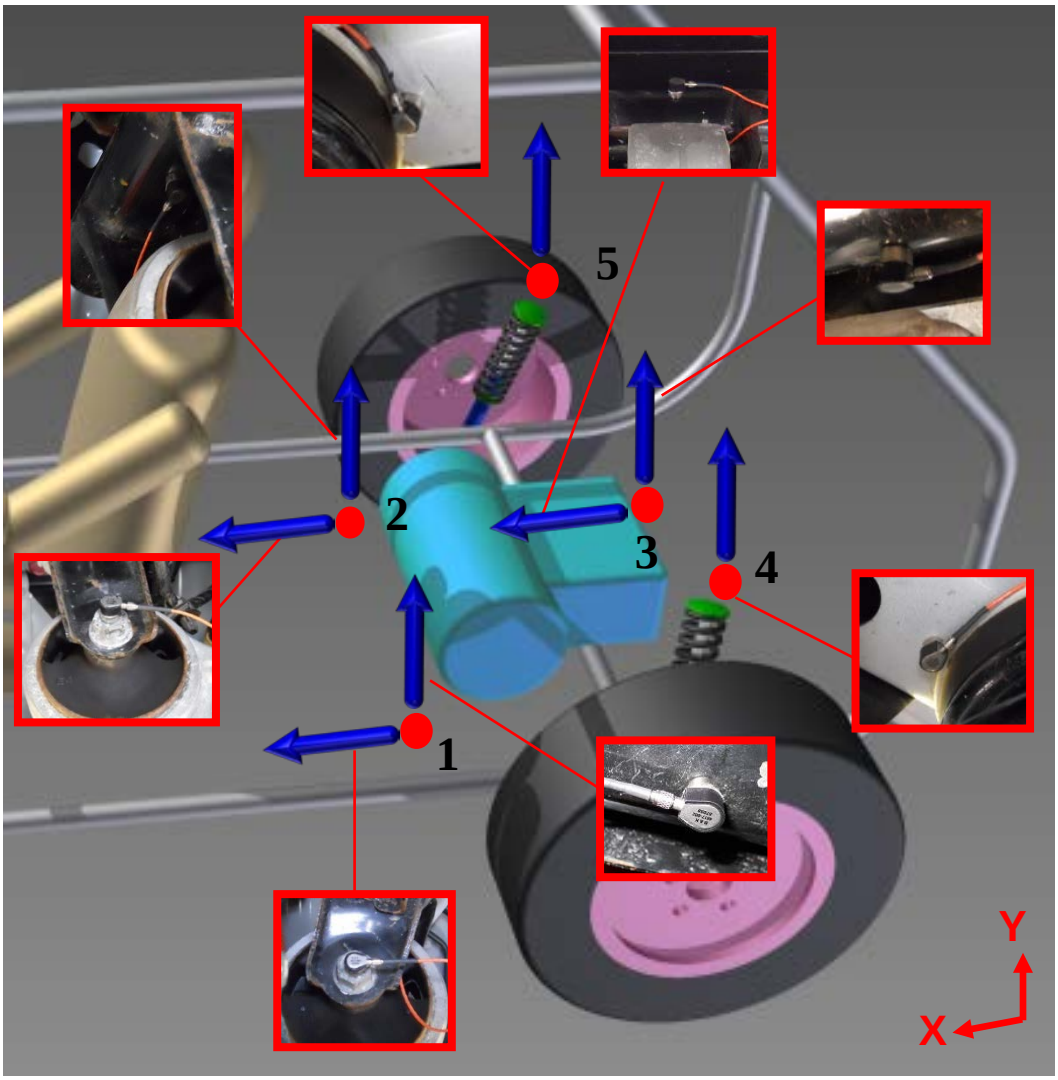

Figure 2 The installed accelerometers and their positions on the vehicle.

Once the accelerometers were installed, the next step was the microphone installation inside the car. This was positioned according to the relevant ISO norm 5128:1980 (Harrison, 2004) near the driver's ear position (Figure 3).

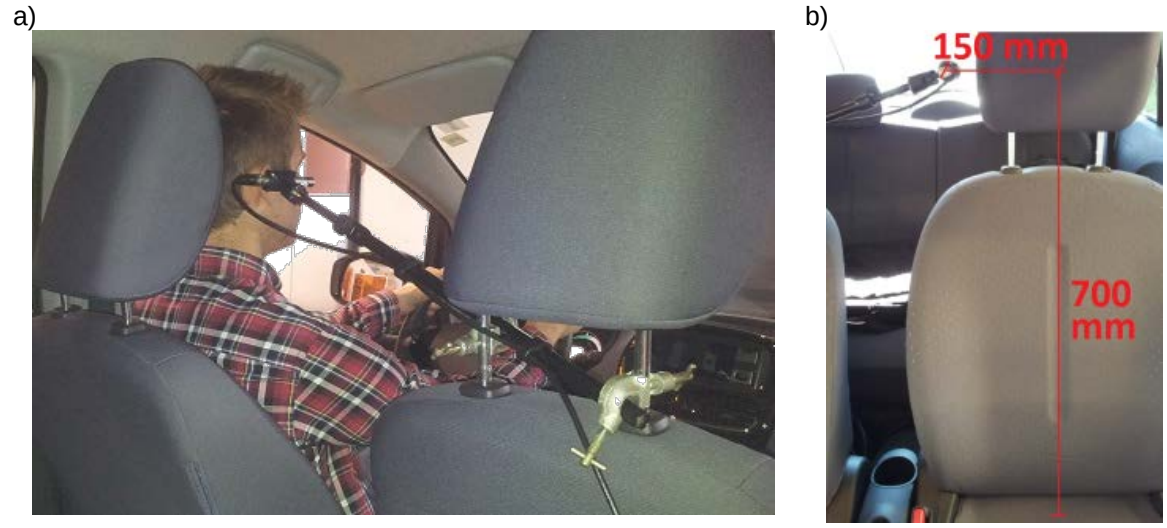

Figure 3 The microphone location near the driver's ear: a) vehicle interior; and b) location relative to driver's seat.

In order to perform the TPA, it was necessary to have the relation between the applied forces and accelerations in the considered locations (later called acceleration-to-force FRF). This is the reason why hammer tests were performed at this stage of the work. Furthermore, acoustic pressure data were collected during these tests in order to calculate the force-to-acoustic-pressure FRF used in later stages. All the gathered impact data had an average coherence between the impact and response greater than 0.9, as shown in Figure 4. To carry out the test and collect data, a LabVIEW script was built to first visualize the test measurements and second to export the data into a file which could be read by Matlab.

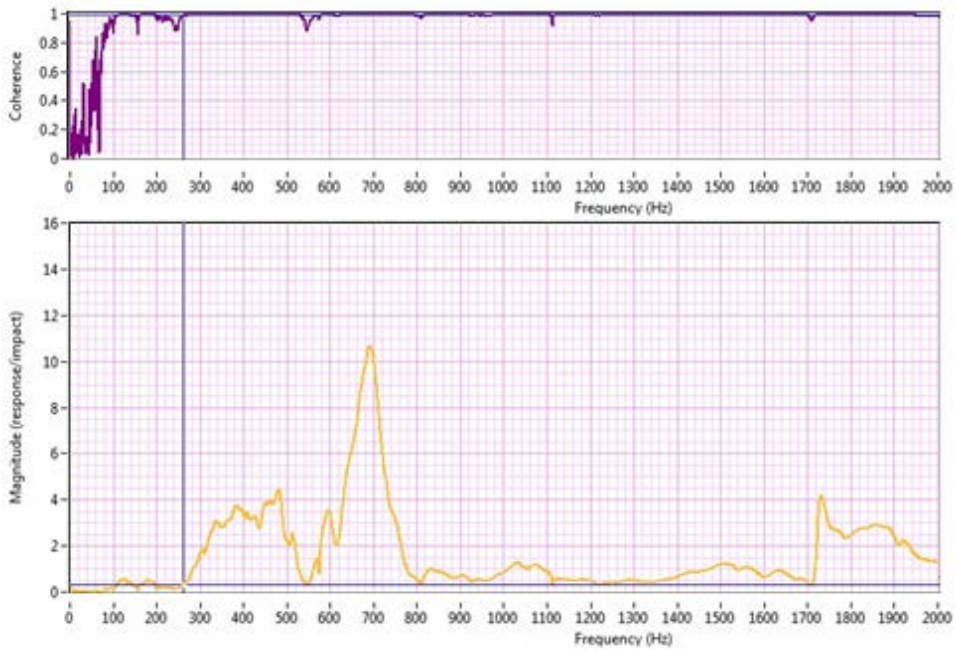

Figure 4 Static FRF impact tests: an example of the measured FRF with the accelerance amplitude at the bottom and the corresponding coherence at the top.

After the static tests were performed, the electric vehicle was installed on the roller bench (chassis dynamometer) to initiate the operational tests (Figure 5 and Figure 6). These tests comprised a vehicle run-up from 0 to 100 km/h whilst measuring the accelerations and acoustic pressure. As it can be seen in Figure 6,

three different regions can be distinguished: the first of which corresponds to the run-up interval; the second of which is almost a stationary region; and the third of which corresponds to the run-down interval. In this study, only the first region was used to calculate the results. The other two regions were analysed to check the correct behaviour of the model, meaning that the behaviour in the run-up period has to be consistent with the behaviour in the run-down period. The whole test was constrained to last one minute because of two reasons: first, it takes some time to accelerate the vehicle up to 100 km/h; and second, the sample frequency was 5 kHz, which means that if the tests lasted more than one minute, the exported data files would be too large to handle (bigger than 1 Gb).

a)

b)

Figure 5 Photographs of the electric vehicle mounted on the chassis dynamometer (roller bench): a) vehicle in the laboratory; and b) the rear wheel on the rollers.

The facilities used to perform the tests were a non-anechoic roller bench (Figure 5) and a non-anechoic bay lift. These limitations naturally led to inaccuracies by not considering the exterior noise as an acoustic source. In this study, although airborne paths were not considered, the exterior sound level was measured (lower than 45 dB(A)) in order to have an estimate of the magnitude of the error likely to occur by not considering it.

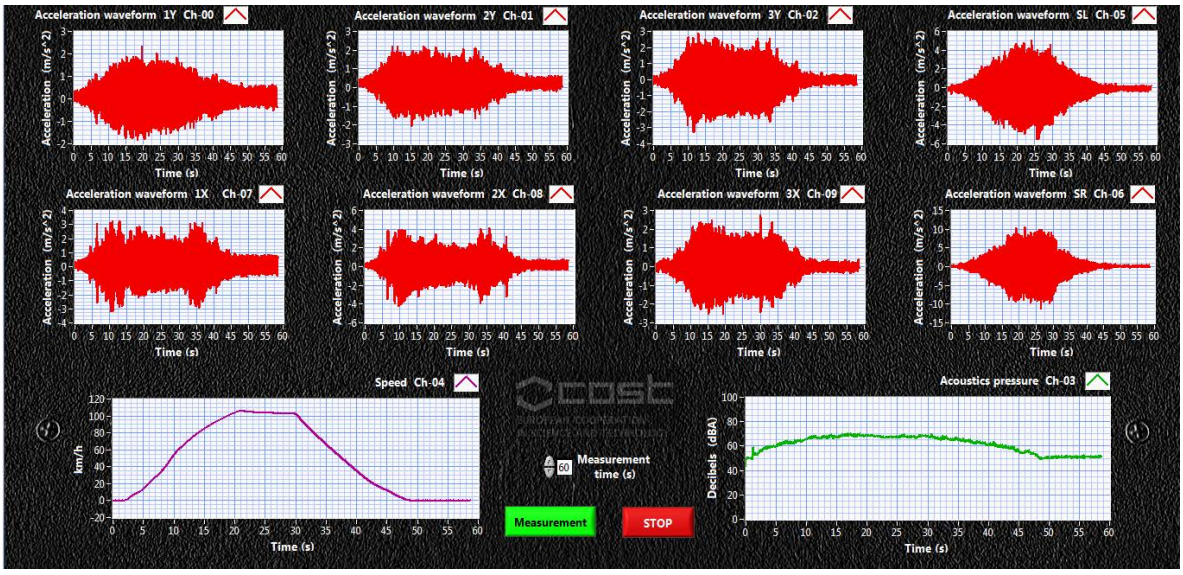

Figure 6 Example of the data gathered in LabView environment during an operational test between 0-60 s: the 8 acceleration signals are displayed at the top; the speed of the car is displayed at the bottom left; and the sound pressure level in dB(A) at the driver's ear is provided at bottom right.

4. Results and discussion

In this section, the OPA and TPA results and a comparison between the two methods are presented. First, an assessment of the accelerometer measurements was done in order to correlate them in terms of modal frequencies and their orders with available past experimental results.

4.1. Correlation with past results

Based on the mechanical setup of the EV, a preliminary analysis focusing on the identification of the natural frequencies and the main excited orders was performed. According to these results, three resonances were expected, one in the region between 200 and 250 Hz, one between 600 and 650 Hz and another between 700 and 800 Hz. All three expected resonances were captured by accelerometers located in different positions and directions in the EV and Figure 7 shows an example from the engine mount 2 vertical accelerometer signal.

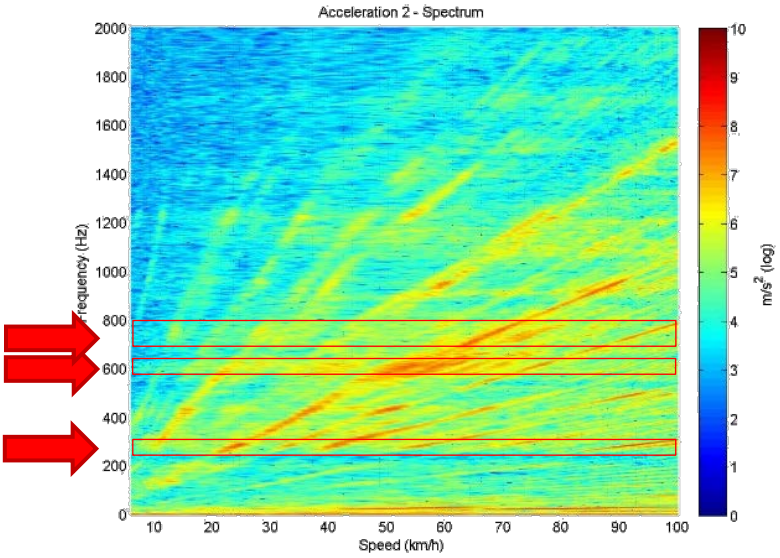

Figure 7 Short Time Fourier Transform (STFT) for the signal from accelerometer 2Y.

Regarding the signal harmonics, seven orders were expected. Two of them (order 0.16 and 0.49) represent the first and third harmonics of the wheel rotation (respectively), three of them are related to the electric motor rotation (order 1) and its construction technology (order 8 is related to the number of rotor poles and order 48 is related to the stator coils) and two of them (order 10.71 and 25) refer to the gearbox. These orders are referred to the electric motor rotation as can be extracted. In order to explain some of these order numbers, a description of the layout of the transmission is necessary. The transmission consists of two helical gears pairs. The first pair is composed by a 25-tooth pinion and a 42-tooth wheel, whilst the second consist of an 18-tooth pinion, which is located in the same shaft as the wheel of the first pair, and a 65-tooth wheel.

Table 2 Harmonics due to the transmission.

Name of the harmonic	Gear ratio	Harmonic number
Harmonic of the first pair pinion	25	25
Harmonic of the second pair pinion	(25 / 42) x 18	10,71
Harmonic of the output (wheel)	(25 / 42) x (18 / 65)	0,16

Figure 8 shows the predicted orders which can be found in the results of the run-up tests.

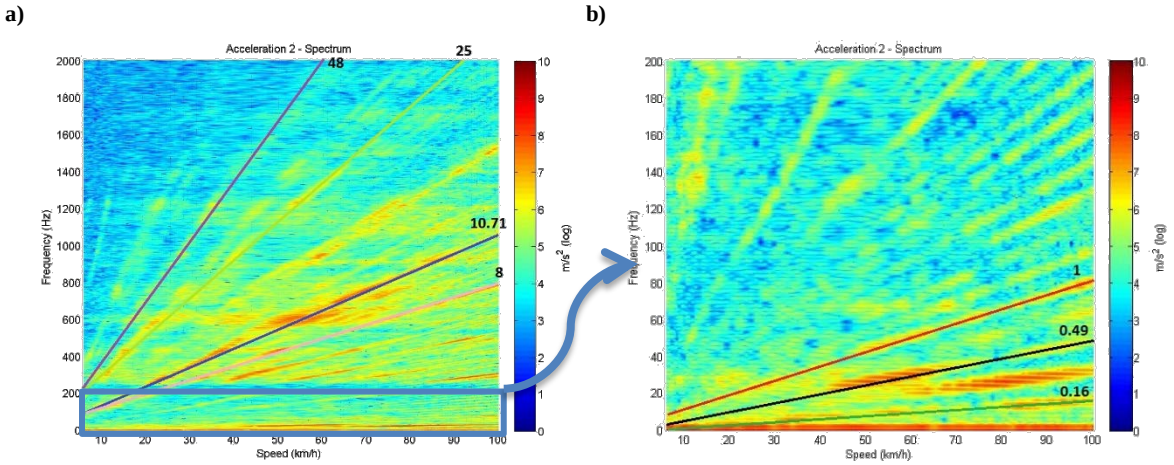

Figure 8 STFT illustrations of the engine orders for the signal from accelerometer 2Y: a) 0 to 2000 Hz; and b) 0 to 200 Hz.

Although the other channels have not been shown for the sake of brevity, similar results were obtained by post-processing all the acquired signals.

4.2. Operational path analysis (OPA)

In this subsection, the results derived from the OPA are shown and assessed. The procedure followed to obtain these results is presented in the flowchart of Figure 9. The methodology comprises of post-processing and assessment of two different operational tests. Using the first test data, the transmissibility functions are calculated by applying equation (3) and then, with the second operational test measurements and transmissibility functions, the acoustic pressure is obtained by means of equation (3) again. The procedure is now illustrated using data from the EV measurements.

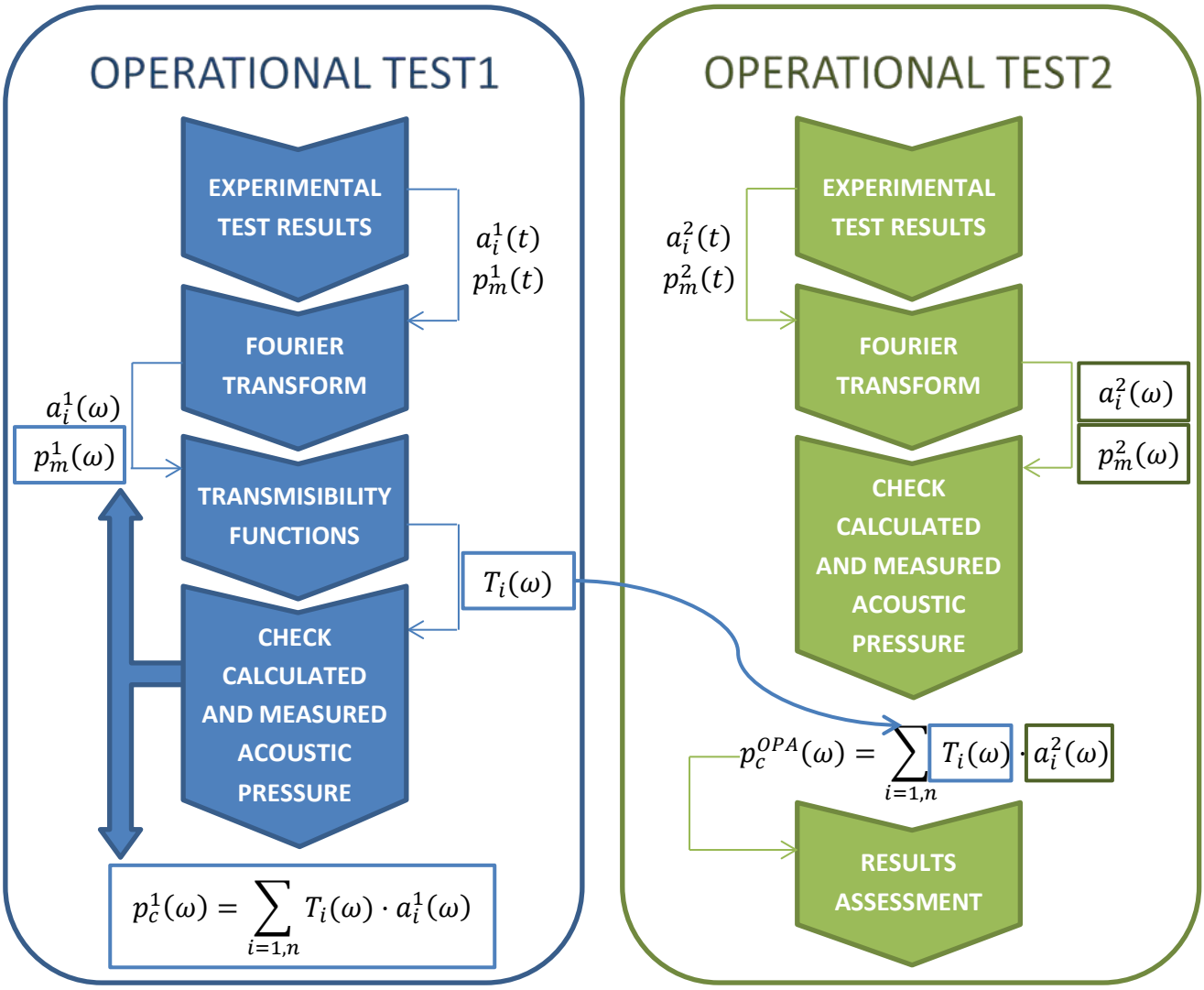

Figure 9 Flow diagrams illustrating the procedure for Operational Path Analysis (OPA).

First, test data was gathered ($a_i^1(t)$ and $p_m^1(t)$) and transformed to the frequency domain ($a_i^1(\omega)$ and $p_m^1(\omega)$), where *i* is the path number (*i=1,n* and *n=8*), subscripts *m* and *c* denote measured and computed, respectively, and the superscript *1* and *2* denotes the test number. The transmissibility functions ($T_i(\omega)$) were then calculated using the H_1 estimator method. In order to check the accuracy and validity of the acquired mathematical results, two different tasks were completed. First, using the transmissibility functions and the measured accelerations, the acoustic pressure was calculated ($p_c^1(\omega)$) and was compared with the measured signal ($p_m^1(\omega)$)). As can be seen in Figure 10, both spectra have a good agreement as expected, since the mathematical procedure is based on assigning to the considered paths the measured acoustic pressure.

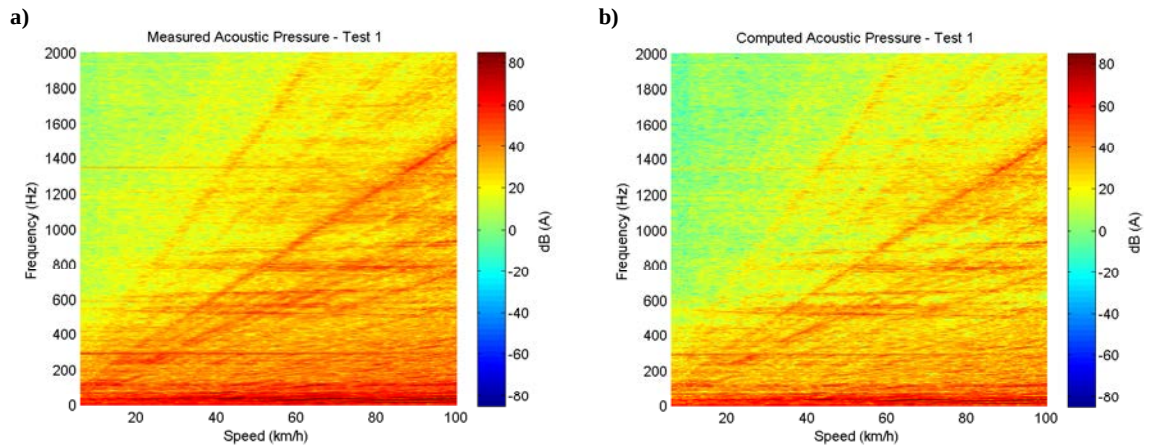

Figure 10 STFT showing the sound pressure level in dB(A) near the driver's ear position with respect to frequency and vehicle speed: a) measured; and b) calculated using the OPA procedure 1.

Ideally, the transmissibility functions must represent the real behaviour of the car transfer paths not only for the test which was used to calculate them, but also for every subsequent operational test. Therefore, a second operational test was performed to check the general applicability of the transmissibility functions. The second test data was gathered ($a_i^2(t)$ and $p_m^2(t)$) and transformed to frequency domain ($a_i^2(\omega)$ and $p_m^2(\omega)$), obtaining finally the acoustic pressure ($p_c^{OPA}(\omega)$) by means of multiplying the second test accelerations by the transmissibility functions obtained in test 1 as illustrated in Figure 9. Once the acoustic pressure was calculated, it was compared with the measured signal from the second operational test ($p_m^2(t)$). As can be seen in Figure 11, similar results are obtained regarding the acoustic levels in the whole frequency and speed range. Some discrepancies can be seen though in the higher frequency range (>1000 Hz) and at low speeds (<30 km/h).

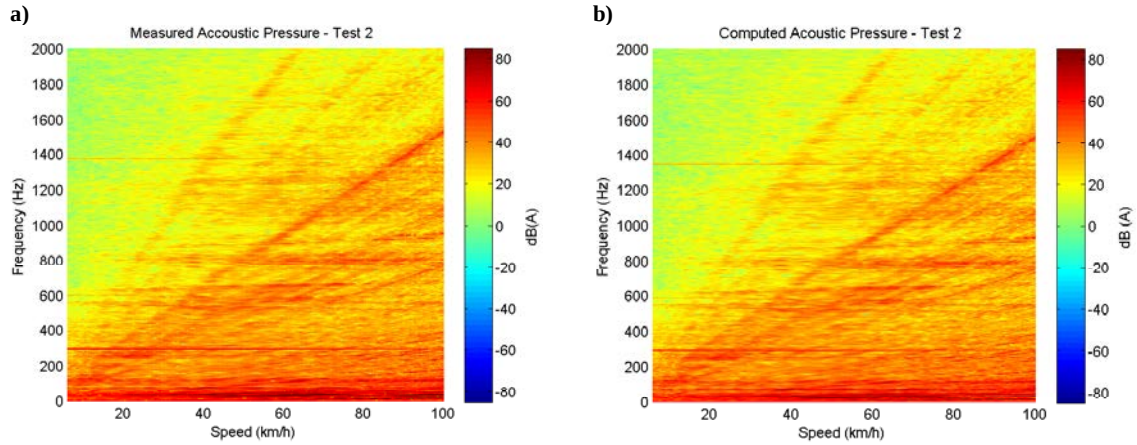

Figure 11 STFT showing the sound pressure level in dB(A) near the driver's ear position against frequency and vehicle speed: a) measured; and b) calculated using the OPA procedure 2.

Once the methodology validation stage is complete, two different sets of results were obtained. The former represents the equivalent noise transmitted through each path (Figure 12 and Figure 13) and the latter is the equivalent noise of all the paths for each powertrain order of interest, represented by the partial path contribution plot (Figure 14). In Figure 14, each row shows the partial contribution of a single path to the target response as a function of the vehicle speed for a given engine order (Gajdatsy et al., 2010). The partial contribution of a single path in OPA is the measured acceleration of the path multiplied by its corresponding transmissibility function, whilst in TPA it is the load multiplied by its corresponding load-to-acoustic pressure FRF.

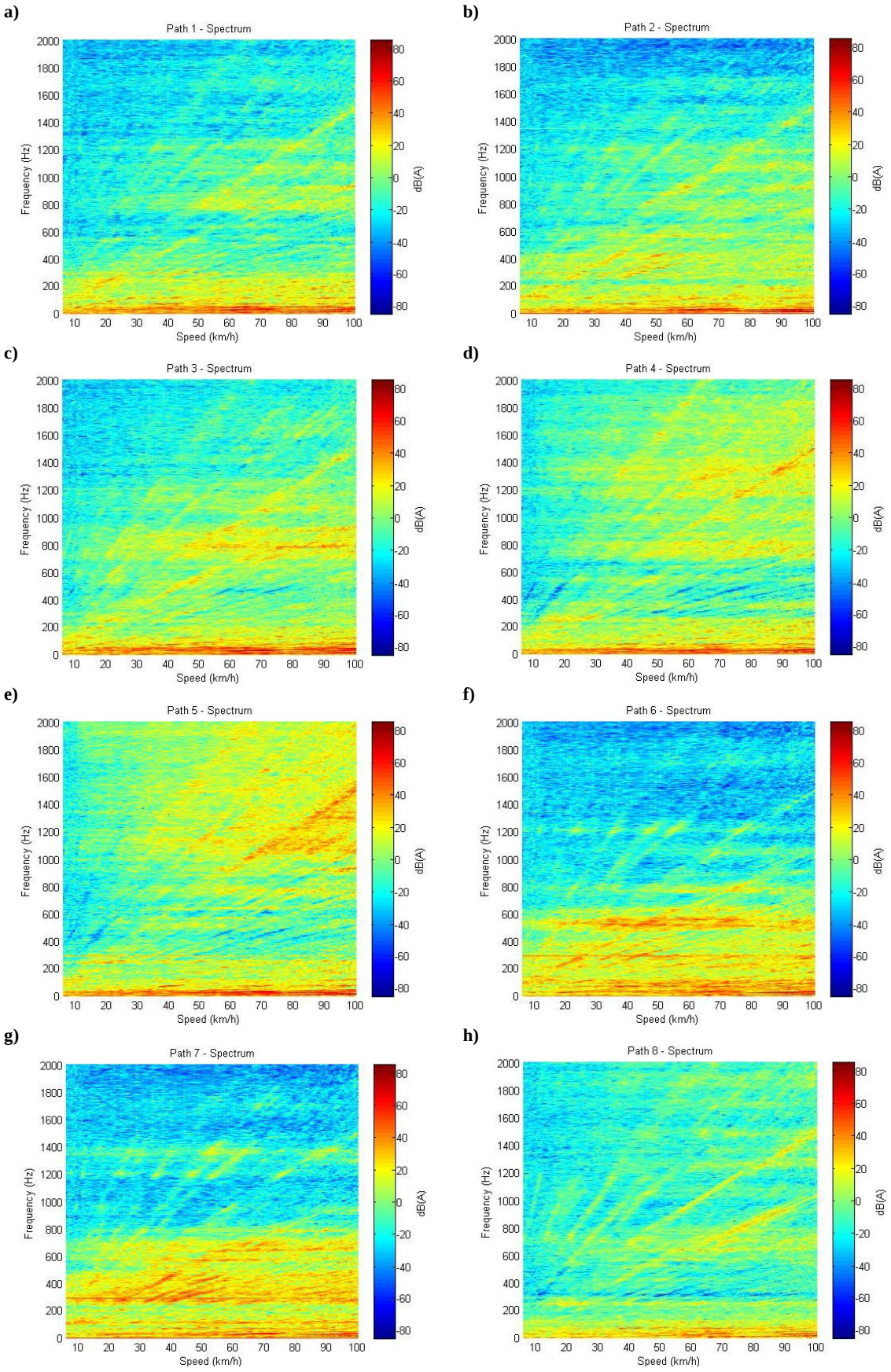

Figure 12 STFT's showing the sound pressure level in dB(A) due to each transfer path against frequency and vehicle speed: a) 1st path; b) 2nd path; c) 3rd path; d) 4th path; e) 5th path; f) 6th path; g) 7th path; and h) 8th path.

From the results shown in Figure 12, it can be appreciated that depending on the frequency range, different noise contributions should be expected. Analysing Figure 12, two different limit frequencies are observed because of a change in each path's impact at (500 and 1000 Hz). For this reason the assessment can be categorised in three different regions: i) low frequencies, below 500 Hz; ii) medium frequencies, between 500-1000 Hz; and iii) high frequencies, above 1000 Hz.

Regarding these three frequency regions and assessing the different path contribution, several conclusions can be reached. With regard to the low frequency region, almost all the paths have an important role. Nevertheless, the 6th and 7th paths have a prominent role in this range. This means that the X direction has a higher contribution than the Y direction. With respect to the medium frequency region, the 3rd, 6th and 7th paths transmit most of the noise. Regarding the last frequency range, mainly the 4th and 5th paths transmit the noise to the cabin. Thus, it can be extracted from the results that the paths related to the motor have a major role in the low and medium frequency ranges, whilst the suspension paths are responsible for the vibrations in the high frequency range. The assessment of the results is summarized in Figure 13, in which the different locations and noise contributions are pictured. The colour of the arrows corresponds to the indicated dB scale.

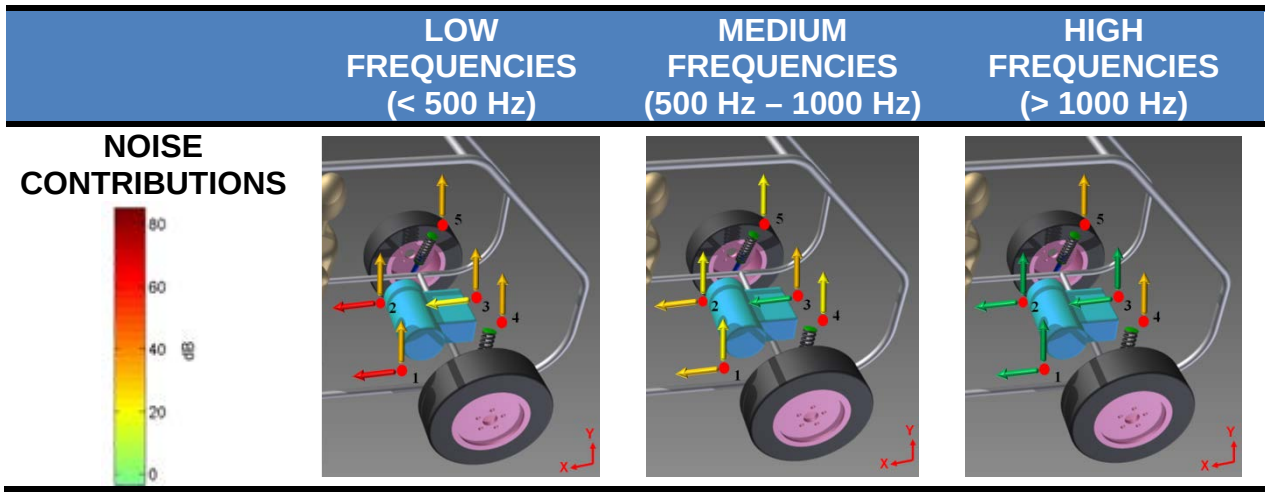

Figure 13 Summary illustrations of the relative strength of each path in the low, medium and high frequency ranges, as calculated using OPA.

From the second set of results, the assessment of the paths' noise contribution for each order of interest is conducted. This is performed by extracting the noise contribution from each path (from the first set of results) for a specific frequency/speed ratio. As in the former set of results, it can be appreciated that depending on the speed region, different behaviour in terms of which path is more prominent was observed (Figure 14). Thus, three different speed regions were studied: i) low speed region, which covers the 0-30 km/h range; ii) medium speed region, from 30-80 km/h; and iii) high speed region, encompassing the 80-100 km/h range.

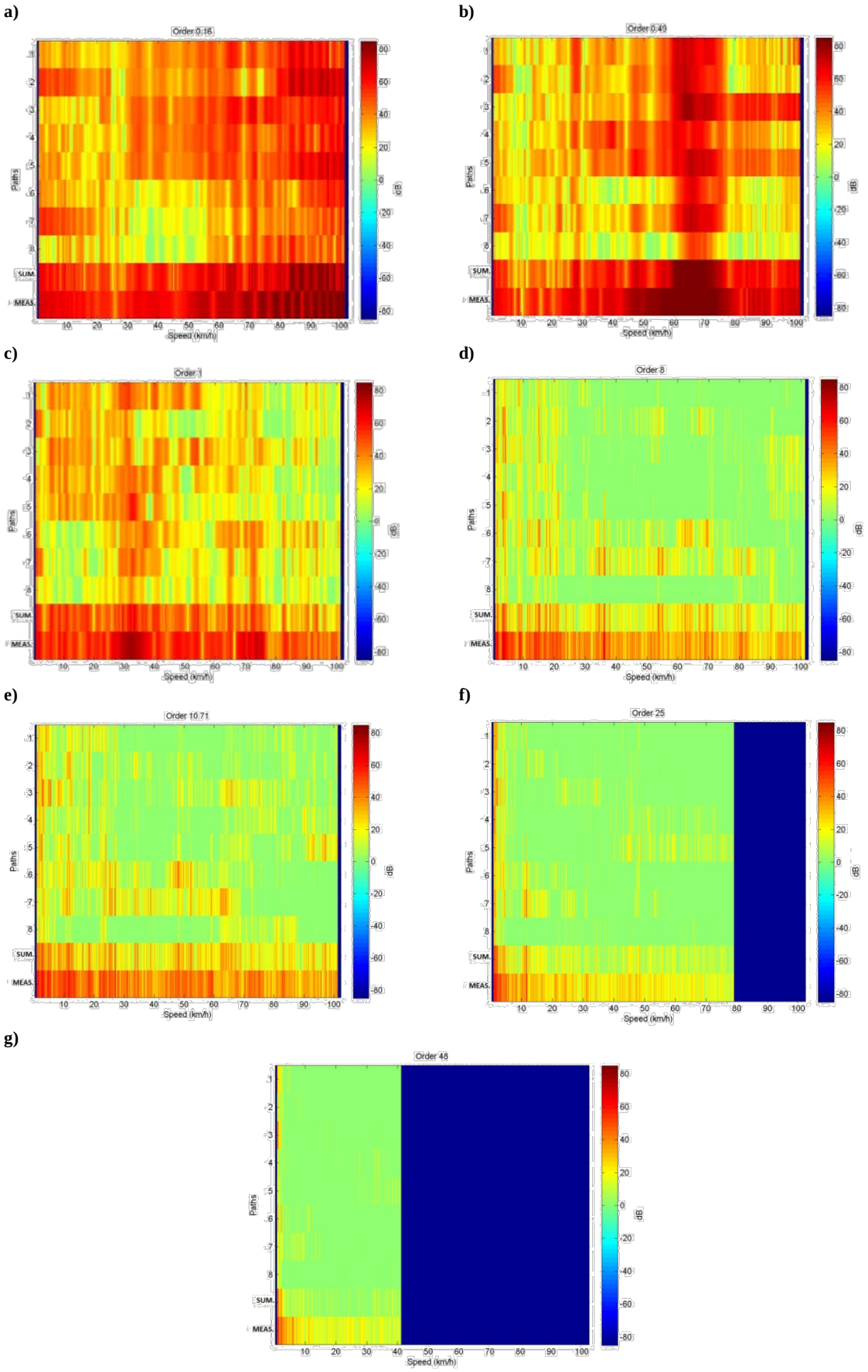

Figure 14 STFT's showing the OPA calculated sound pressure levels (SPL) due to each path (1 to 8) as well as the calculated total SPL ("sum") and the total measured SPL ("meas") at the dominant engine orders: a) order 0.16; b) order 0.49; c) order 1; d) order 8; e) order 10.71; f) order 25; and g) order 48.

An assessment summary is shown in Figure 15, where the most prominent paths depending on the speed region are exhibited for each order of interest. The colour of the arrows corresponds to the indicated dB scale.

Figure 15 Summary illustrations of the relative strength of each path (1 to 8) calculated using OPA at the dominant engine orders in the low, medium and high speed ranges.

From Figure 15 some general conclusions can be extracted. It can be seen that the motor source is more important than the suspension in the low speed region for all the orders, whilst the suspension paths have a

higher impact in the high speed region. In the medium speed region, the suspension paths may have a higher effect on the acoustic level than the electric motor paths depending on the order of interest. Specifically, in the orders lower than 10.71, the motor paths are more prominent than the suspension ones, the contrary if the case when the order is higher than 25. Moreover, the Y direction is more important generally than the X direction in almost all the orders and speed regions.

4.3. Transfer path analysis (TPA)

In this third subsection, the TPA results are to be presented and assessed. The procedure followed is presented in the flowchart of Figure 16. The methodology comprises the post-processing of two different tests: static impact tests; and dynamic operational tests. From the impact test data, the FRFs, first between accelerations and forces and second between forces, and acoustic pressures were measured. Then, with these FRFs and the operational test measurements, the acoustic pressure is calculated by applying the inverse matrix method (equations (1) and (2)). A summary of the procedure is illustrated in Figure 16 using the measured EV data^{o}, where i is the path number ($i=1,n$ and $n=8$), subscripts m and c denote the measured and computed, respectively, and the superscripts h and 2 denote the hammer test and the operational test number, respectively.

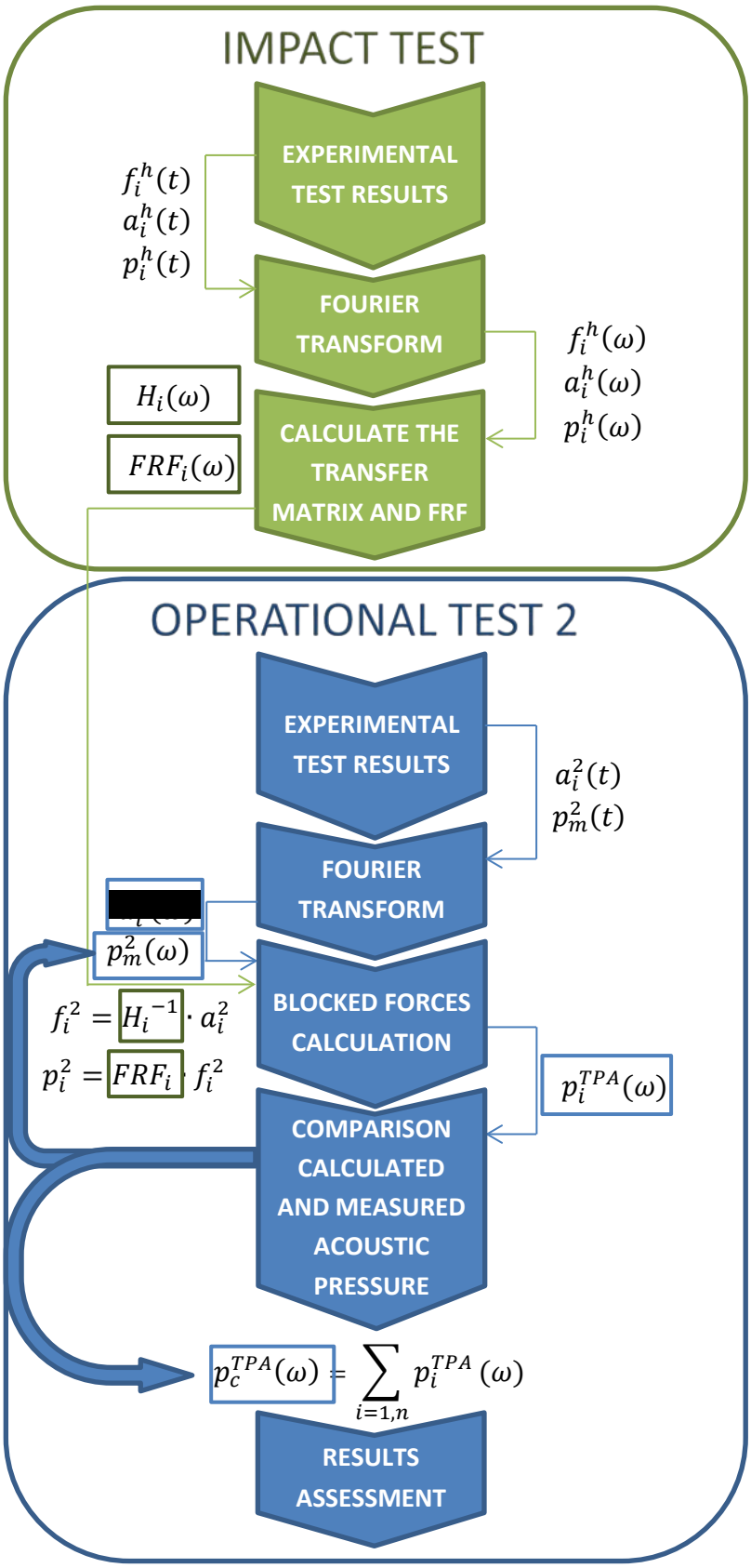

Figure 16 Flowchart illustrating the procedure for Transfer Path Analysis (TPA).

Several impact tests were performed in each point of interest (ten in each location and direction). From these tests, five impact tests were collected randomly in order to calculate the mean FRFs. In each impact test,

accelerations in all the points ($a_i^h(t)$), the applied force ($f_i^h(t)$) and the acoustic pressure in the cabin ($p_i^h(t)$) were measured, where superscript *h* denotes the hammer test. With the acceleration and force data transformed to frequency domain ($a_i^h(\omega)$ and $f_i^h(\omega)$) and applying the inverse matrix method for each frequency, the transfer matrix between forces and accelerations was calculated ($H_i(\omega)$). Moreover, the FRFs between forces and acoustic pressure for each path ($FRF_i(\omega)$) was determined with a similar procedure but using $f_i^h(\omega)$ and $p_i^h(\omega)$.

Once both the FRFs (acceleration-to-force transfer matrix and force-to-acoustic pressure matrix FRFs) were computed, the operational test data was collected and transformed to frequency domain, $a_i^2(\omega)$ and $p_m^2(\omega)$ (the same operational test as in the OPA method was used in order to compare the results). Then, the conversion of the operational accelerations to equivalent blocked forces (f_i^2) was performed, by means of the acceleration-force matrix ($H_i(\omega)$). With these blocked operational forces and the corresponding $FRF_i(\omega)$, the equivalent acoustic pressure transmitted by each path ($p_i^{TPA}(\omega)$) was calculated. Furthermore, adding all the considered paths, the equivalent acoustic pressure in the cabin was computed ($p_c^{TPA}(\omega)$) and compared with the measured one ($p_m^2(\omega)$). As can be seen in Figure 17, the agreement between both spectra is not very good in the high frequency range (above 1000 Hz). This indicates that there are missing sources or missing paths in the high frequency range. Nevertheless, although the agreement is not perfect, the versatility of the method has been demonstrated since a larger number of sources or paths can be considered without varying the methodology.

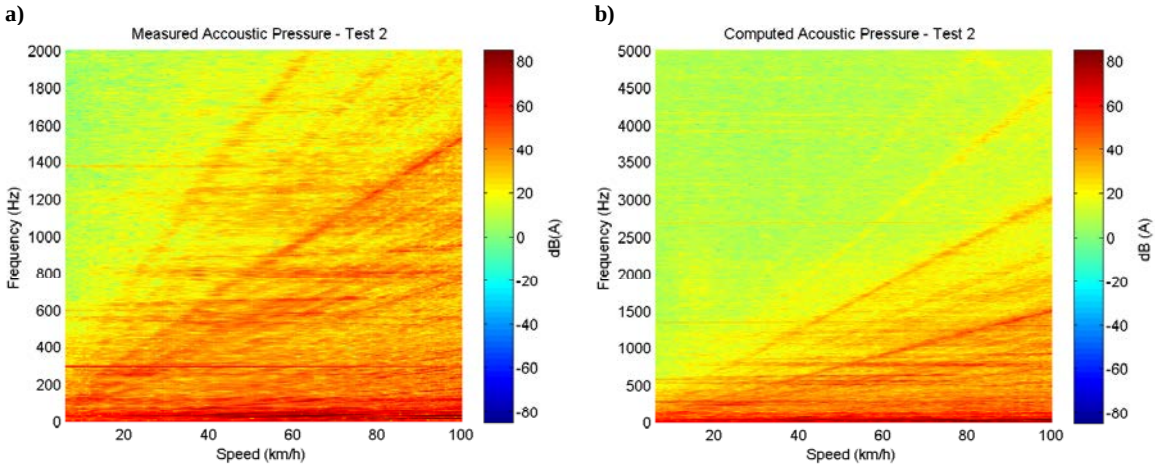

Figure 17 STFT showing the sound pressure level in dB(A) near the driver's ear against frequency and vehicle speed: a) measured SPL; and b) calculated SPL using TPA.

Once the validation stage is completed, two different sets of results are presented. The former represents the equivalent noise that each path is transmitting to the cabin (Figure 18 and Figure 19) and the latter is the equivalent noise of all the paths in the orders of interest, which is represented by the partial path contribution plot (Figure 20).

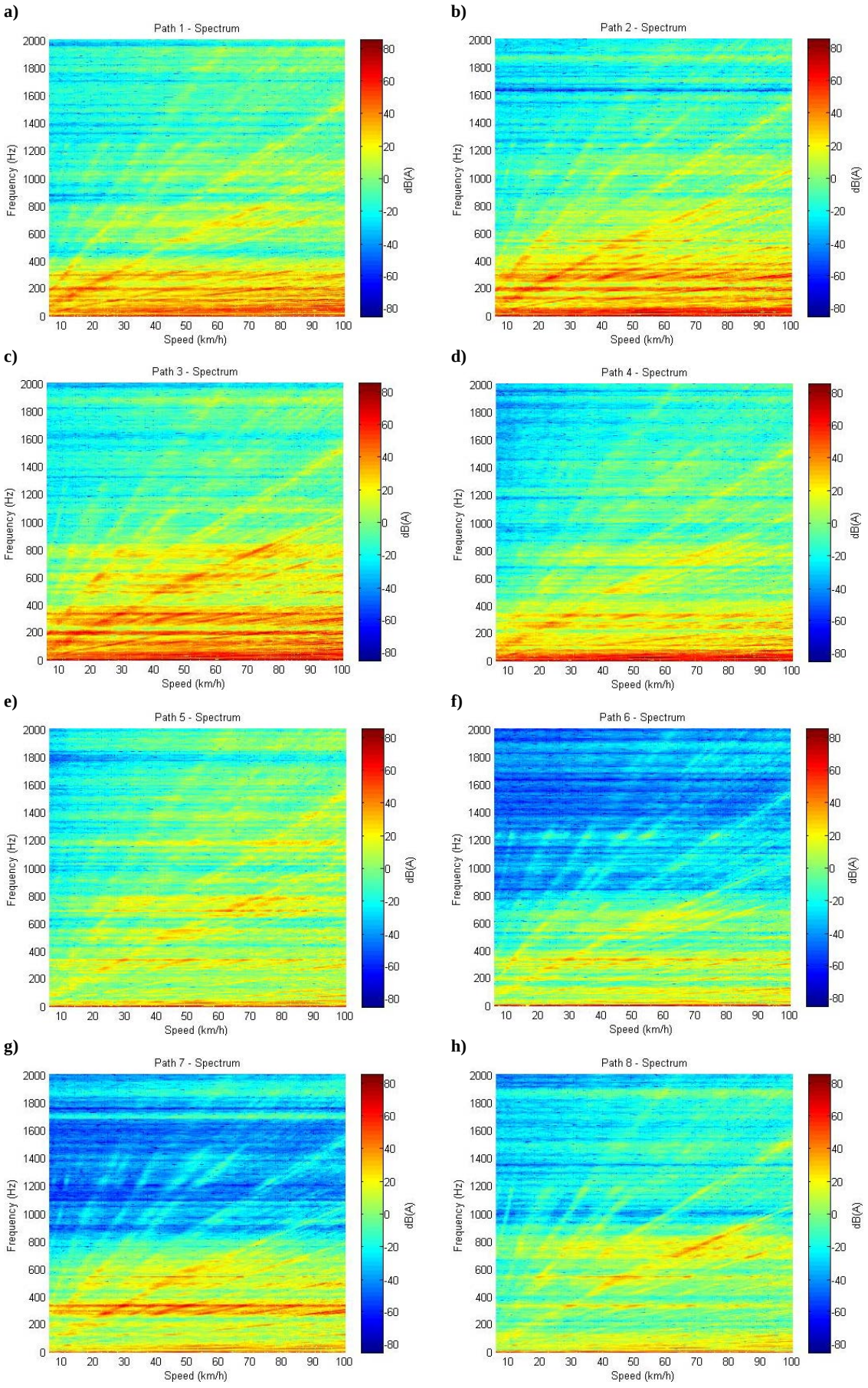

Figure 18 STFT showing the sound pressure level in dB(A) due to each transfer path against frequency and vehicle speed calculated using TPA: a) 1st path; b) 2nd path; c) 3rd path; d) 4th path; e) 5th path; f) 6th path; g) 7th path; and h) 8th path.

From the above mentioned set of results, the same evaluation as in the OPA method assessment was conducted in order to investigate which paths are transmitting the noise to the cabin and assess what is their impact. With this information, it can be determined which paths have a higher effect within a specific range of frequencies.

As commented in the previous subsection, depending on the range of frequencies considered, a different noise contribution is expected per path. When analysing the behaviour of these noise contributions, the same three frequency regions were considered: i) low frequencies (< 500 Hz); ii) medium frequencies (500-1000 Hz); and iii) high frequencies (> 1000 Hz).Regarding these three regions and assessing the contribution from different paths, the following conclusions can be reached. With regard to the low frequency region, almost all the paths have an important role. Nevertheless, the 1st to 4th and the 7th paths have a prominent role in this range. With respect to the medium frequency region, all the paths have similar contribution, with the 3rd being the most important. Regarding the high frequency region, the 4th and 5th paths convey the most noise to the cabin, nevertheless the impact is low. It can therefore be concluded that the electric motor paths have a major impact in the low and medium frequency ranges, whilst the suspensions are the elements transmitting most vibrations in the higher frequency range. The assessment of these results is summarized in Figure 19.

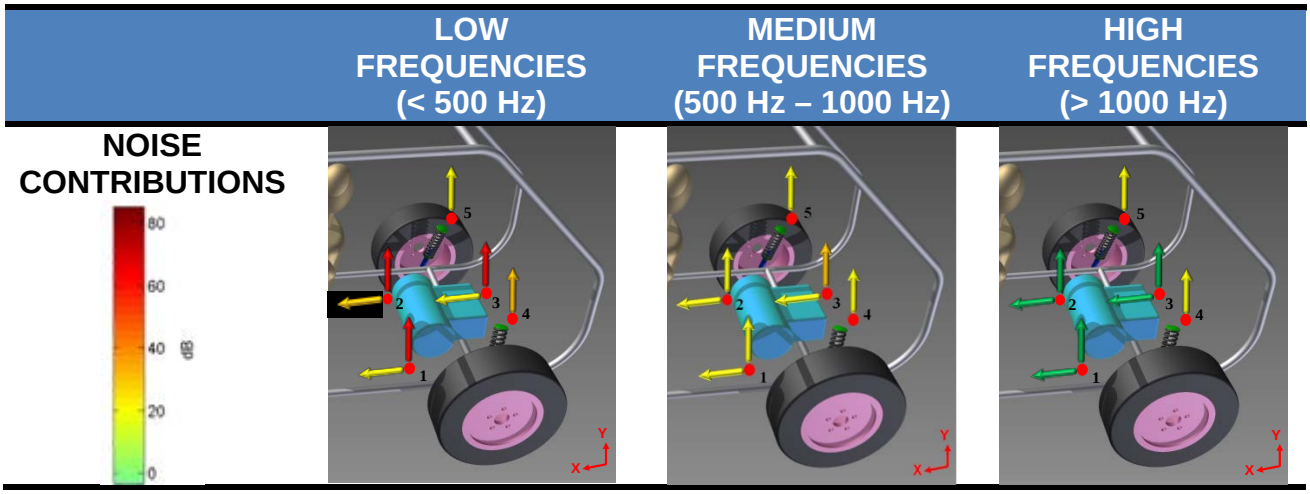

Figure 19 Summary Illustrations of the contribution of each path in the low, medium and high frequency ranges calculated using TPA.

From the second set of results (Figure 20), the assessment of the paths' noise contribution for each order of interest is conducted. This is performed by extracting the noise contribution from each path for a specific frequency/speed ratio. As in the OPA case, it can be appreciated that depending on the speed region, different prominent paths are expected. Thus, three different regions were studied: i) low speed region (0-30 km/h); ii) medium speed region (30-80 km/h); and iii) High speed region (80-100 km/h).

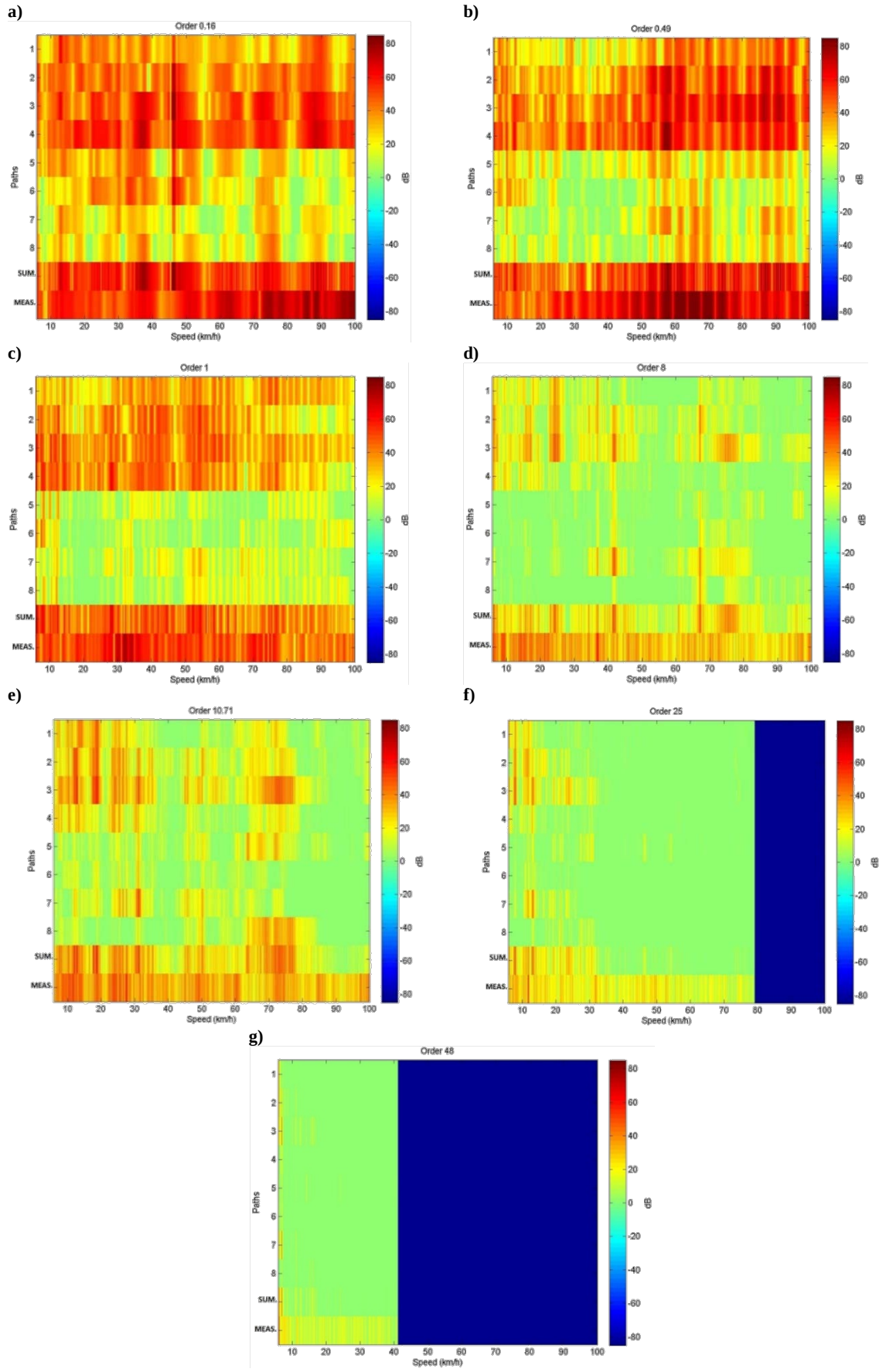

Figure 20 STFT's showing the TPA calculated sound pressure levels (SPL) due to each path (1 to 8), as well as the calculated total SPL ("sum") and the total measured SPL ("meas") at the dominant engine orders: a) order 0.16; b) order 0.49; c) order 1; d) order 8; e) order 10.71; f) order 25; and g) order 48.

For the sake of visual clarity, in Figure 21 an assessment summary of the second set of results is presented, where the most prominent paths (depending on the speed region) for each order of interest are shown.

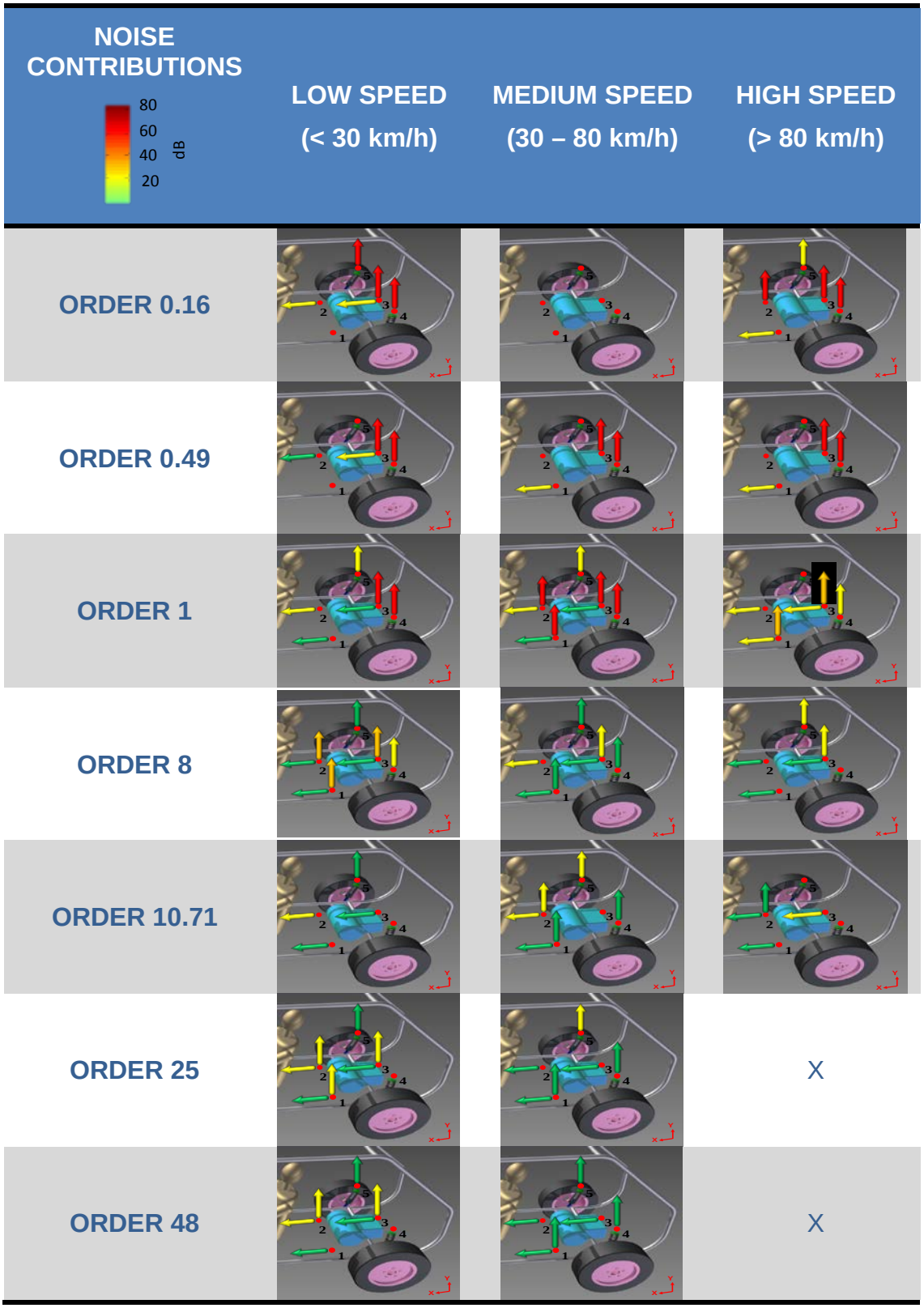

Figure 21 Summary illustrations of the relative contribution of each path (1 to 8) calculated using the TPA at the dominant engine orders in the low, medium and high speed ranges.

From Figure 21 some general conclusions can be drawn. It can be seen that it is not clear that the electric motor paths are more important than the suspension in the low speed region for all the orders, however it is clear for the higher orders (25^{th} and 48^{th}). A similar behaviour can be observed in the other two speed regions. Thus, suspension or motor paths can be important depending on the order assessed. What is clear is that the Y direction is more important than the X direction in almost all the orders and speed regions.

4.4. Comparison between OPA and TPA

In this section, a comparison between the two methods is presented. First, the main differences regarding the methodologies are explained and last, the main differences among the results produced by each method are described.

With regard to the methodology, several dissimilarities can be found. Whilst in OPA, only operational tests are necessary to execute the method, in TPA, both operational and static tests are required (in this case impact tests). In the OPA method, as the transmissibility functions are obtained by the measured acoustic pressure, other operational tests are needed to check the validity of these functions. Nonetheless, in TPA, as the system properties (acceleration-to-force and force-to-acoustic pressure FRFs) are calculated by static tests, only one operational test is required for validation. Moreover, whilst the OPA mathematical method uses the measured acoustic pressure in operational conditions to obtain the transmissibility functions, TPA does not employ this to calculate the properties of the system. This fact could lead to an error if all the main sources and paths are not considered, meaning that, in the OPA case, the mathematical procedure computes noise contributions to the considered paths which do not belong to them in reality if the path which carries the real noise impact is not considered. In the TPA case, if all the paths are not considered, there will be a discrepancy between the measured and the computed acoustic pressure due to the fact that the real noise impact is taken into account.

These methodology differences lead to different computed acoustic pressures for both methods. This can be appreciated in Figure 11 and Figure 17, where the computed and measured acoustic pressures are shown. Specifically, what can be observed is that the OPA acoustic pressure agrees better with the measured sound pressure level than for the TPA case. Nevertheless, this does not mean that the OPA method performs better than the TPA method, it means that more paths have to be taken into account. The main discrepancy between measured and computed acoustic pressures is observed in the high frequency range (above 1000 Hz). This leads to the conclusion that the OPA method is assigning some acoustic impact to the considered paths which is produced in reality by other sources and paths (this is why it is not observed in the TPA case).

Furthermore, in order to identify the similarities and dissimilarities between both OPA and TPA methods, the results regarding their paths' contribution have been compared (i.e. Figure 12 versus Figure 18). From this assessment, it can be appreciated that there are some magnitude discrepancies between both methods, where TPA results are higher than the OPA results, nevertheless, both method results follow a similar trend under 1000 Hz. It can be seen that this trend changes in the high frequency region (above 1000 Hz), especially in the 4^{th} and 5^{th} paths, that correspond to the suspension. The OPA calculation suggests that in the high frequencies a significant contribution arises from the suspension paths, whilst the TPA results indicate that this is not the real behaviour. It seems that the TPA results are more reliable than the OPA results in this case, since the mathematical calculation of the OPA method assigns this impact to the paths which are more prone to transmitting these noise frequencies. As a general conclusion, it was inferred that TPA results are more reliable

than OPA ones. Nevertheless, even if quantitatively the methods disagree, qualitatively they lead to the same solution which is that the electric motor source has a major impact in the low and medium frequency ranges, whilst the suspension paths are the elements transmitting vibrations in the higher frequency range.

From the assessment of the results presented in Figure 13 and Figure 19 regarding the noise impact in the orders of interest, similarities between both methods can be found. It can be appreciated that in both methods the paths which contribute to the noise in the cabin in each frequency range are the same. Moreover, although quantitatively they are not equal, qualitatively their impacts are similar. This means that even though the two methods lead to different values of acoustic pressure in the corresponding paths, the path importance tendency is the same in both methods. In the low frequency region, it can be observed that 1st, 2nd and 3rd paths are more significant in the TPA results than in the OPA results, whilst in the 5th, 6th and the 7th paths the impact is lower. As explained in the OPA subsection, the TPA results are the expected ones. Thus, it means that the Y direction is predominant in this frequency range. In the medium frequency range, the 6th and 7th path contributions are higher in OPA than in TPA. Furthermore, this behaviour remains the case in the high frequency range, which means that 4th and 5th path contributions are higher in OPA than in TPA.

From Figure 14 and Figure 20, a comparison between TPA and OPA results for acoustic pressure impact of each path regarding the orders of interest can be made and is shown in Figure 22. This figure presents the differences between the TPA and OPA results by showing the TPA results and marking the similarities (✓) and discrepancies (×) against corresponding the OPA results. Although there is some discrepancy, a qualitative agreement can be noticed. Moreover, from a comparison of the results (OPA and TPA) in all the considered orders, 6 out of 8 paths agree between the two methods as inferred from Figure 22.

Figure 22 Contribution of each path (1 to 8) calculated using the TPA and agreement (✓) and discrepancies (✖) with the corresponding OPA result at the dominant engine orders in the low, medium and high frequency ranges.

5. Conclusions

Transfer Path Analysis and Operational Path Analysis were performed on an electric vehicle and the results were presented in this study. A comparison between both methods taking into account the eight structure-borne paths from the engine and the suspension points to the vehicle cabin has been presented. One of the aims of this study is to check the versatility of these two methods, commonly used in petrol and diesel engine cars. Beyond this goal, the additional aim of this work is to assess which paths are transmitting vibrations from the electric vehicle sources to the driver's ear. For both OPA and TPA, two different sets of results have been presented: i) the noise contribution spectrum of each path; and ii) the path noise impact for some harmonic orders which arise due to the physical components of the electric vehicle. In the former case, three different frequency regions have been analysed in order to determine which paths are critical under these conditions. In the latter case, three speed regions have been analysed in order to determine which paths are critical in each order.

A comparison of the measured with the predicted interior noise from the TPA method (Figure 17) showed good qualitative similarity but indicated that not all the relevant paths were considered in the analysis. A comparison of the predicted OPA data with the corresponding predicted TPA data for each path indicated that below 1000 Hz the OPA method generally identified the correct frequency content in each path, however, the magnitudes of the data were often different.

In general, with respect to which paths are transmitting most of the noise to the cabin, the electric motor paths have a major impact in the low and medium frequency range, whilst the suspensions are the elements transmitting most vibrations in the higher frequency range. However, as noted above, the magnitudes of the contributions predicted by the OPA method may be in error because of the limited number of paths considered.

Regarding the versatility of the two methods when applied to an EV, one of the conclusions extracted from this study is that OPA results give a qualitative approximation and can be obtained within a short period of time, whilst to obtain the TPA results is a longer and more laborious procedure. Hence, if preliminary results are to be calculated, the OPA method can be suitable. For example, although it can be expected that a higher number of transfer paths will produce more accurate results, a good agreement against vehicle cabin measurements of acoustic pressure has been obtained in the low and medium frequencies (less than 1000 Hz) by using only eight paths. Thus, if a preliminary assessment in low frequency regions is required, a small number of paths would suffice to obtain satisfactory results.

Nonetheless, if more accurate results are expected, a more extensive TPA method is required. If not, distorted results are obtained in the OPA case and incomplete results are gathered in the TPA case.

Acknowledgements

The authors would like to acknowledge the COST ACTION TU 1105 for supporting this research.

References

Ahlersmeyer, T. (2009). Transfer path analysis - a review of 18 years of practical application. Rotterdam, The Netherlands.

Chan, C. C. (1993). Overview of electric vehicle technology. *Proceedings of the IEEE, 81*(9), 1202-1213.

Chan, C. C. (2002). The state of the art of electric and hybrid vehicles. *Proceedings of the IEEE, 90*(2), 247-275.

De Klerk, D., & Ossipov, A. (2010). Operational transfer path analysis: Theory, guidelines and tire noise application. *Mechanical Systems and Signal Processing, 24*(7), 1950-1962.

De Klerk, D., & Rixen, D. J. (2010). Component transfer path analysis method with compensation for test bench dynamics. *Mechanical Systems and Signal Processing, 24*(6), 1693-1710.

De Sitter, G., Devriendt, C., Guillaume, P., & Pruyt, E. (2010). Operational transfer path analysis. *Mechanical Systems and Signal Processing, 24*(2), 416-431.

DeLuchi, M. A. (1989). Hydrogen vehicles: An evaluation of fuel storage, performance, safety, environmental impacts, and cost. *International Journal of Hydrogen Energy, 14*(2), 81-130.

Elliott, A. S., Moorhouse, A. T., Huntley, T., & Tate, S. (2013). In-situ source path contribution analysis of structure borne road noise. *Journal of Sound and Vibration, 332*(24), 6276-6295.

El-Refaie, A. M. (2011). Motors/generators for traction/propulsion applications: A review. *2011 IEEE International Electric Machines and Drives Conference, IEMDC 2011,* Ontario, Canada. 490-497.

Fukuo, K., Fujimura, A., Saito, M., Tsunoda, K., & Takiguchi, S. (2001). Development of the ultra-low-fuel-consumption hybrid car - INSIGHT. *JSAE Review, 22*(1), 95-103.

Gajdatsy, P., Gielen, L., Janssens, K., Van Der Auweraer, H., Mas, P., & Desmet, W. (2009). A novel TPA method using parametric load models: Validation on experimental and industrial cases. *SAE Technical Paper 2009-01-2165,* doi:10.4271/2009-01-2165

Gajdatsy, P., Janssens, K., Desmet, W., & Van Der Auweraer, H. (2010). Application of the transmissibility concept in transfer path analysis. *Mechanical Systems and Signal Processing, 24*(7), 1963-1976.

Gaudin, A., & Gagliardini, L. (2007). Recent improvements in road noise control. *SAE Technical Papers 2007-01-2358,* doi: 10.4271/2007-01-2358

Guasch, O., García, C., Jové, J., & Artís, P. (2013). Experimental validation of the direct transmissibility approach to classical transfer path analysis on a mechanical setup. *Mechanical Systems and Signal Processing, 37*(1-2), 353-369.

Harrison, M. (2004). *Vehicle refinement: Controlling noise and vibration in road vehicles*. Oxford: Elsevier Science & Technology.

Janssens, K., & Britte, L. (2012). Pass-by noise TPA. *International Conference on Noise and Vibration Engineering 2012, ISMA 2012, Including USD 2012: International Conference on Uncertainty in Structure Dynamics,* Leuven, Belgium. *, 2* 1567-1572.

Janssens, K., Gajdatsy, P., Gielen, L., Mas, P., Britte, L., Desmet, W., & Van Der Auweraer, H. (2011). OPAX: A new transfer path analysis method based on parametric load models. *Mechanical Systems and Signal Processing, 25*(4), 1321-1338.

Judd, S. L., & Overbye, T. J. (2008). An evaluation of PHEV contributions to power system disturbances and economics. *40th North American Power Symposium, NAPS2008,* Calgary, Canada. doi:10.1109/NAPS.2008.5307393

Lennström, D., Johnsson, R., Agren, A., & Nykänen, A. (2014). The influence of the acoustic transfer functions on the estimated interior noise from an electric rear axle drive. *SAE International Journal of Passenger Cars - Mechanical Systems, 7*(1), 413-422.

Lennström, D., Olsson, M., Wullens, F., & Nykänen, A. (2016). Validation of the blocked force method for various boundary conditions for automotive source characterization. *Applied Acoustics, 102,* 108-119. doi:10.1016/j.apacoust.2015.08.019

Magrans, F. X. (1981). Method of measuring transmission paths. *Journal of Sound and Vibration, 74*(3), 321-330.

Magrans, F. X. (1993). Definition and calculation of transmission paths within an S.E.A. framework. *Journal of Sound and Vibration, 165*(2), 277-283.

Maia, N. M. M., Silva, J. M. M., & Ribeiro, A. M. R. (2001). Transmissibility concept in multi-degree-of-freedom systems. *Mechanical Systems and Signal Processing, 15*(1), 129-137.

Moorhouse, A. T., Elliott, A. S., & Evans, T. A. (2009). In situ measurement of the blocked force of structure-borne sound sources. *Journal of Sound and Vibration, 325*(4–5), 679-685. doi:http://dx.doi.org/10.1016/j.jsv.2009.04.035

Official Journal of the European Communities. (1991). Council directive of 26 june 1991 amending directive 70/220/EEC on the approximation of the laws of the member states relating to measures to be taken against air pollution by emissions from motor vehicles (91/441/EEC), (1991).

Official Journal of the European Communities. (1994). Directive 94/12/EC of the european parliament and the council of 23 march 1994 relating to measures to be taken against air pollution by emissions from motor vehicles and amending directive 70/220/EEC.

Official Journal of the European Communities. (2002). Commission directive 2002/80/EC of 3 October 2002 adapting to technical progress council directive 70/220/EEC relating to measures to be taken against air pollution by emissions from motor vehicles.

Official Journal of the European Union. (2007). Regulation (EC) no 715/2007 of the european parliament and the council of 20 june 2007 on type approval of motor vehicles with respect to emissions from light passenger and commercial vehicles (euro 5 and euro 6) and on access to vehicle repair and maintenance information.

Official Journal of the European Union. (2008). Commission regulation (EC) No 692/2008 of 18 July 2008 implementing and amending regulation (EC) No 715/2007 of the european parliament and of the council on type-approval of motor vehicles with respect to emissions from light passenger and commercial vehicles (euro 5 and euro 6) and on access to vehicle repair and maintenance information (1), (2008).

Padilha, P. E. F., & De Frana Arruda, J. R. (2006). Comparison of estimation techniques for vibro-acoustic transfer path analysis. *Shock and Vibration, 13*(4-5), 459-467.

Plunt, J. (2005). Finding and fixing vehicle NVH problems with transfer path analysis. *Sound and Vibration, 39*(11), 12-16.

Taymaz, I., & Benli, M. (2014). Emissions and fuel economy for a hybrid vehicle. *Fuel, 115*, 812-817.

Thanapalan, K. K. T., Kim, J. R., Carr, S. J. W., Zhang, F., Premier, G. C., Maddy, J., & Guwy, A. J. (2011). Progress in the development of renewable hydrogen vehicles, storage, infrastructure in the UK: Hydrogen centre in its early years of operation. *Proceedings of the 2nd International Conference on Intelligent Control and Information Processing, ICICIP 2011*, Harbin Institute of Technology Harbin, China. (PART 2) 738-742.

Van den Bosch, D. D., Van der Seijs, M. V., & de Klerk, D. (2014). Validation of blocked-force transfer path analysis with compensation for test bench dynamics. *Dynamics of coupled structures, volume 1: Proceedings of the 32nd IMAC, A conference and exposition on structural dynamics, 2014* (pp. 37-49) Springer International Publishing. doi:10.1007/978-3-319-04501-6_4

Van der Seijs, M. V., de Klerk, D., & Rixen, D. J. (2016). General framework for transfer path analysis: History, theory and classification of techniques. *Mechanical Systems and Signal Processing, 68–69*, 217-244. doi:http://dx.doi.org/10.1016/j.ymssp.2015.08.004